ACS APPLIED MATERIALS & INTERFACES

Research Article

www.acsami.org

Improved Methanol Barrier Property of Nafion Hybrid Membrane by Incorporating Nanofibrous Interlayer Self-Immobilized with High Level of Phosphotungstic Acid

Ebrahim Abouzari-lotf,*[,†,‡] Mohamed Mahmoud Nasef,[†,‡] Hossein Ghassemi,[⊥] Masoumeh Zakeri,[†,‡] Arshad Ahmad,[‡] and Yadollah Abdollahi[§]

[‡]Advanced Materials Research Group, Institute of Hydrogen Energy, Universiti Teknologi Malaysia, International Campus, 54100 Kuala Lumpur, Malaysia

[†]Malaysia−Japan International Institute of Technology, Universiti Teknologi Malaysia, 54100 Kuala Lumpur, Malaysia

[⊥]Department of Macromolecular Science & Engineering, Case Western Reserve University, 44106-7202 Cleveland, Ohio United States

[§]Department of Electrical Engineering, Faculty of Engineering, University of Malaya, 50603 Kuala Lumpur, Malaysia

S *Supporting Information*

ABSTRACT: High level of phosphotungstic acid (PWA) was self-immobilized on electrospun nylon nanofiberous sheet to fabricate highly selective methanol barrier layer for sandwich structured proton conducting membranes. Simple tuning for the assembly conditions of central layer and thickness of outer Nafion layers allowed obtaining different composite membranes with superior methanol barrier properties (namely, $P = 3.59 \times 10^{-8}$ cm^2 s^{-1}) coupled with proton conductivities reaching 58.6 mS cm^{-1} at 30 °C. Comparable activation energy for proton transport and more than 20 times higher selectivity than Nafion 115 confirm the effectiveness of the central layer and resulting membranes for application in direct methanol fuel cells (DMFCs). When tested in DMFC single cell, the performance of hybrid membrane was far better than Nafion 115 especially at higher methanol concentrations.

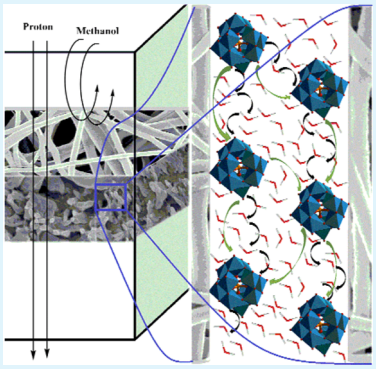

KEYWORDS: *self-immobilized materials, electrospun nanofibers, phosphotungstic acid, composite membranes, proton transfer*

INTRODUCTION

The advances in proton exchange membranes (PEM)s is critical for improving the performance of electrochemical energy systems including polymer-ion and redox flow batteries (RFB), electrolyzers, and fuel cells.[1−3] Since PEMs have different functions of separating the reactants and conducting the protons while electrically insulating, the membranes should meet the characteristic of high ionic conductivity, low fuel/charge crossover, and sufficient mechanical stability. Typically, even though perfluorinated sulfonic acid membranes showed exceptional proton conductivity upon employing in DMFCs, excess methanol permeability ensue fuel loss as well as lower energy efficiency and fuel cell performance. Using of diluted feed (<4 M of methanol) which is frequently supposed to minimize such excessive permeability is likely to reduce the energy density of fuel cell significantly.[4]

The ultimate solution to such high crossover, which is a key barrier for the development of DMFC, PEMFC, and RFB technologies, is the utilization of membranes with low feed/water/electrolyte crossover. Various strategies and materials have been developed to mitigate this issue without causing any concomitant loss in either proton conductivity or stability.[1,4,5] In this light, using of polymers with low intrinsic crossover and introducing inorganic proton conductor materials such as heteropoly acids (HPA)s have been considered extensively. An interesting class of materials for suppressing methanol permeability is the polymers containing basic groups including amine, amide, imine, and imidazole.[6,7] One of the key membranes of interest in DMFC is PBI-based materials, such as commercialized Celtec-V membrane, which is a blend of PBI and polyvinylphosphonic acid.[8] Although some encouraging results were reported,[9] the conductivity is low and need to be improved.

Hybrid organic−inorganic substrates have been used to enhance the conductivity of polymers thru introducing solid proton transport materials in the flexible polymer matrix.[10,11] Several fabrication methods adopted for the preparation of hybrid organic−inorganic substrates including dip-coating, spray-coating, doctor blading, electrospinning, and electrochemical deposition.[12] Among all, electrospinning has attained a remarkable interest for films because of its ability to produce substrates with highly porous structure, small pore size, and

Received: March 15, 2015
Accepted: July 21, 2015
Published: July 21, 2015

DOI: 10.1021/acsami.5b02268
ACS Appl. Mater. Interfaces 2015, 7, 17008−17015

high surface-to-volume ratio.[13] The technique is flexible and could be used to prepare nanofibers from wide range of highly conductive polymers, including Nafion,[14,15] reinforced Nafion,[16,17] sulfonated aromatic polymer,[18,19] and porous scaffold for preparation of layer-by-layer membranes.[20] On the other hand, the technique was successfully used to produce diverse range of hybrid organic−inorganic proton conductor substrates for fuel cell applications.[21−24] However, most fillers used for these membranes lack protogenic groups, which resulting in low proton conductivity.

HPAs (such as phosphotungstic acid $H_3PW_{12}O_{40}$, PWA) have a very strong Brønsted acidity approaching the superacid region (more acidic than 100% sulfuric acid and Nafion) and exhibiting fast reversible redox transformations.[25] PWA has been immobilized in various proton conducting membranes to improve methanol barrier property and/or water retention,[26,27] and enhance the performance at dry conditions and/or elevated temperatures.[28,29] Two different procedures were mainly used to fabricate PWA immobilized materials. The widely used method involves the impregnation of porous substrate,[29,30] or mixing with polymer followed by casting.[31,32] However, although these composite membranes revealed some improved properties, they still suffer from low proton conductivities and leaching out of PWA during the fuel cell operation.[33] Such limitations is due to the low PWA loading level, loose interaction with polymer substrate and agglomeration leading to formation of large particles or clusters during the casting process.[28,34] To overcome this problem, a second method involving copolymerization of PWA containing monomers was proposed.[34,35] The covalent bonding of PWA to the polymer backbone minimizes the risk of PWA leaching and enhances its immobilization level. However, the synthesis procedure is complicated and leads to high processing cost and therefore, the application of this method become limited.

In a recent study, we proposed simple yet efficient route taking the advantages of both methods to enhance the immobilization of PWA toward forming stable layered structure with a negligible leaching out. To avoid the inherent poor mechanical performance of multilayer membranes, the PWA molecules were immobilized onto the nylon-66 electrospun nanofibers, which is known as highly mechanically stable material while showing low methanol permeability.[6,20] It was shown that anchoring high level of PWA increase the proton conductivity of electrospun nanofiberous sheet, for example, 40 wt % of PWA increase the conductivity from 0.82 to 22.87 mS cm^{-1}. Flexible and mechanically stable 3 layered membrane was assembled by sandwiching a central layer composed of high level of PWA between two outer layers of recast Nafion. Typically, a membrane selectivity of 12.6×10^8 mS·s cm^{-3} is achieved which is around 20 times greater than the selectivity of Nafion 115. Such high selectivity has resulted in a power density of 127.1 mW cm^{-2} in a single cell which is 113.3% higher than Nafion 115.

EXPERIMENTAL SECTION

Characterizations. SEM images of composite membranes were obtained on the Philips XL30 field emission scanning electron microscope (FESEM) after coating with 5 nm Au. The cross-sectional morphology were examined using samples cryofractured in liquid nitrogen. Fourier transform-infrared attenuated total reflection (FT-IR-ATR) analysis was performed using Agilent Cary 660 spectrometer. X-ray diffraction pattern was obtained on the Philips X'Pert 1 X-ray diffractometer with graphite monochromatized Cu Kα radiation (λ = 1.5401 Å) at scanning rate of 2°/min over a range of 2θ = 4−80°. Thermogravimetric analysis (TGA) was performed on the PerkinElmer TGA7 under nitrogen atmosphere at a heating rate of 10 °C min^{-1}. The ion exchange capacity was determined via titration procedure as describes earlier.[36] Leaching PWA from the membrane was measured by immersing the composite membranes (size of 2.5 cm × 2.5 cm, volume/weight ratio of around 0.61 cm^3g^{-1}) in 50 mL deionized water at room temperature and monitoring the concentration of PWA in water every 12 h using a UV-1800 UV−vis spectrometer. The chemical stability of the membranes was evaluated by the Fenton test. Preweighed dry membranes (size of 2.5 cm × 2.5 cm) were soaked in a 100 mL Fenton aqueous solution (3% H_2O_2 containing 2 ppm $FeSO_4$) at 80 °C for up to 24h. The stability was evaluated by recording the retained weight of the membranes after complete drying at 80 °C for 12 h in a vacuum oven.

To evaluate the effectiveness of membranes in reducing methanol crossover, the permeability test was conducted using a dual chamber apparatus, where the membrane sample is the separator between ultrapure water and 2 M methanol solution. Both compartments were magnetically stirred at room temperature and the increase in methanol concentration of the receiver compartment as a function of time was monitored by the changes in the methanol concentration using a gas chromatography technique with a FID detector (GC-FID, Agilent, 7820A) and DB-WAX column. The permeability of methanol (P) was calculated from the slope of the plot between the CR and diffusion time (t) with the equation

$$C_R = \frac{A}{V_R}\frac{P}{L}C_0(t - t_0) \quad (1)$$

where C_0 and t_0 are the initial concentration of methanol in the compartment on the left side of the membrane and the time lag, V_R is diffusion reservoir volume, and A and L are the area and thickness of the membrane.

The in-plane and through-plane proton conductivities of the membranes were measured by using a four-point probe of Bekk Tech conductivity cells (BT-112) and two-point probe of homemade stainless steel cylindrical electrodes with diameter of 20 mm (Supporting Information, Figure S1). The resistance of the membranes was measured by using a DC conductivity testing (Keithley 2400 sourcemeter). The potentiostat was set to apply a specific voltage between the two inner probes and measure resulting current. The slop of the data from current versus voltage measurement was used to calculate the resistance (R) and proton conductivity (σ) was calculated according to the equation

$$\sigma\ (\mathrm{S/cm}) = \frac{L\ (\mathrm{cm})}{R\ (\Omega) \times A\ (\mathrm{cm})^2} \quad (2)$$

where L is the distance in the direction of ion flow between voltage measurement probes, A is the area of the membrane, and denominator term of equation, $R\ (\Omega) \times A\ (\mathrm{cm})^2$, describes the area resistance. The activation energy (E_a) of proton conduction was calculated from conductivity−temperature relationship using the Arrhenius equation

$$\sigma = \sigma_0 e^{-E_a/RT} \quad (3)$$

where σ_0 is the pre-exponential factor, R is the universal gas constant (8.314 J mol^{-1} K^{-1}), and T is the absolute temperature in Kelvin.

Membrane water uptake, defined as the difference in mass before and after the complete dryness of the membranes, ϕ_w, was calculated using the equation

$$\phi_w = \frac{W_{wet} - W_{dry}}{W_{dry}} \times 100 \quad (4)$$

where W_{wet} is the weight of the membrane after soaking in water for 24 h and W_{dry} is the weight after complete drying in a vacuum oven at 80 °C for 24 h. Water and methanol uptake was also calculated using the same equation, while W_{wet} was set for the weight of the membrane after soaking in 5 M MeOH for 24 h.

DOI: 10.1021/acsami.5b02268
ACS Appl. Mater. Interfaces 2015, 7, 17008−17015

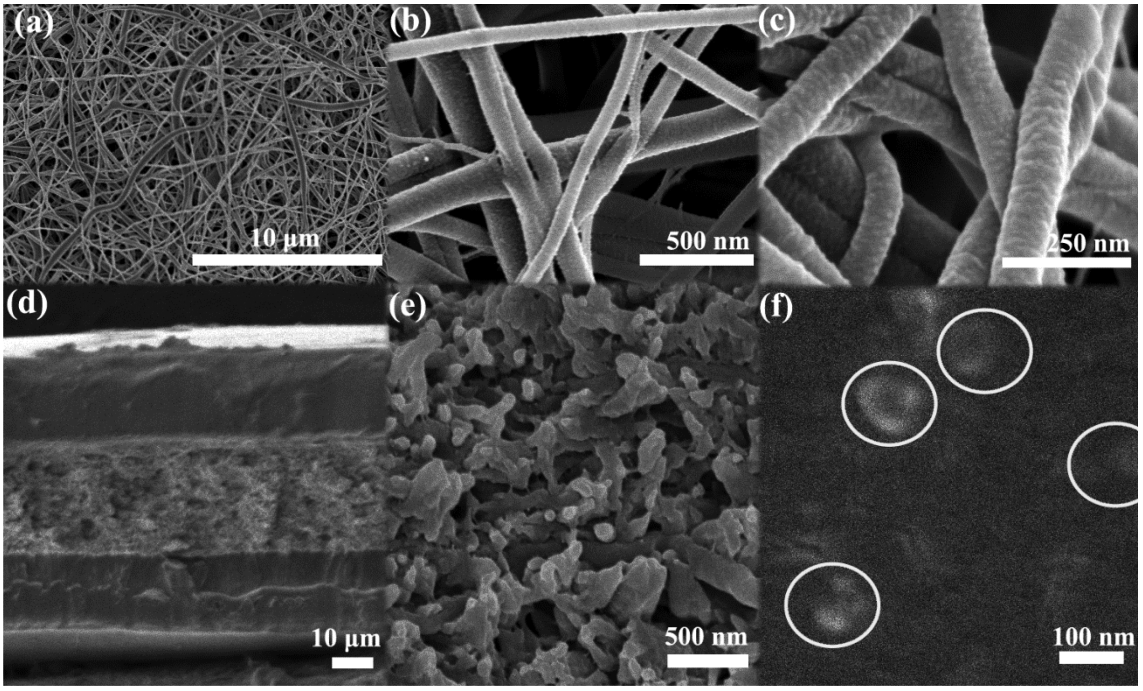

Figure 1. FESEM images of the electrospun mats having average fiber diameter of 85 nm (a) and (b), PWA anchored nanofibers (c), cross-sectional image, which the recast Nafion are the amorphous regions on both sides and the PWA anchored nanofibers is the lighter band in the center (d), and zoom in the central (e) and top layers (f).

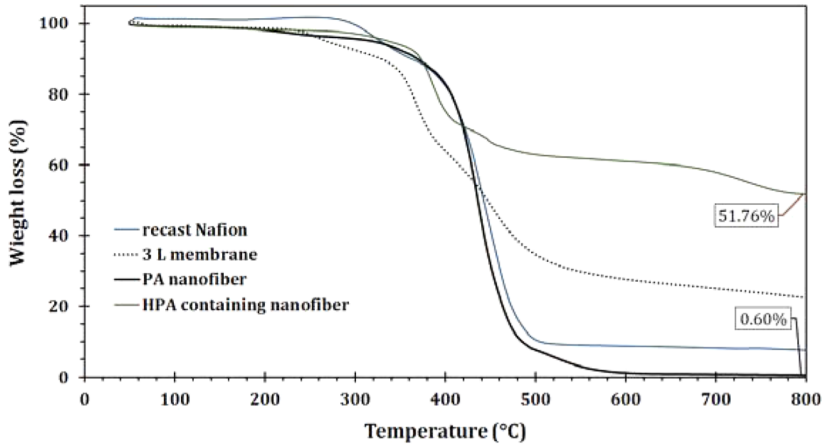

Figure 2. Thermal gravimetric analysis of pristine nylon nanofiber, PWA anchored one, 3 L membrane and recast Nafion. PWA loading level could be calculated from comparison of char yields of pristine nanofiber and HPA anchored one.

Similarly, the in-plane (S_{in}), through-plane (S_{tr}), and volume swelling (S_v) of the membranes in water and 5 M MeOH were calculated using the equation

$$S_x = \frac{X_{wet} - X_{dry}}{X_{dry}} \times 100 \quad (5)$$

where x represents in-plane, through-plane, or volume swelling measurements and X_{wet} and X_{dry} are the length, thickness, or volume of swollen and dry membranes, respectively.

Preparation of Composite Membranes. Electroris (FNM Ltd.) system was utilized to perform electrospinning process of a technical grade nylon-66 (medium viscous, DSM Co., The Netherlands). Electrospinning solution containing 18 wt % of nylon-66 was prepared in a mixture of formic and acetic acids (50/50 wt %) under continuous stirring at room temperature in a glass reactor. The applied voltage was set at 20 kV and the distance between the tip of the metal needle and the aluminum foil collector was set at 12 cm. The flow rate of the polymer solution was controlled by a syringe pump set at 0.4 mL h^{-1} and the collector drum rotation speed was 200 r·min^{-1}. After 10−36 h of electrospinning, the mat with a desired thickness was carefully removed and dried in a vacuum oven for 12 h to completely remove the solvent residues. A series of PWA anchored mats were prepared by the immersion of the prepared nanofiberous sheet in an aqueous solution of PWA of desired concentration (5−20 wt %) at room temperature for different time intervals in range of 1−10 days. The nanofiberous sheet was subsequently removed, washed with plenty of deionized water to remove unbounded molecules, and dried in a vacuum oven at 50 °C overnight.

Thin Nafion layers of desired thickness (25−35 μm) were prepared by casting 15% concentrated aqueous solution of Nafion (5%, supplied from DuPont). Composite membranes containing PWA anchored electrospun mats and two outer recast Nafion layers were mechanically compacted between two ETFE films at above the glass transition of both polymers (130 °C) at 1560 psi for 30s. To enhance the adhesion between layers, Nafion solution was sprayed on the three components

DOI: 10.1021/acsami.5b02268
ACS Appl. Mater. Interfaces 2015, 7, 17008−17015

before assembling. To ensure a uniform compression, the samples were rotated 90° three times. Heat treatment of the membranes was performed at 130 °C for 5 h in a vacuum oven. Finally, the membranes were soaked in 1 N H_2SO_4 for 24 h, rinsed with deionized water and dried in a vacuum oven.

Membrane Electrode Assembly and DMFC Performance. The membranes were pretreated by boiling for 1 h in 3 wt % H_2O_2, deionized water, 1 M H_2SO_4 and finally Milli-Q water. The catalyst ink was prepared by mixing electrocatalysts with 5 wt % of Nafion ionomer (Du Pont) as a binder and water isopropanol (1:1) using ultrasound. Pt/Ru black (1:1) and Pt black were used as electrocatalysts in the anode and cathode, respectively. The catalyst-coated membrane was prepared by spraying the catalyst onto a membrane with a loadings of around 4 mg cm^{-2} for both anode and cathode sides. Membrane electrode assembly (MEA) with an active area of 5 cm^2 was prepared by hot pressing the catalyst-coated membrane with carbon paper at 130 °C under 1300 psi for 5 min and tested with DMFC hardware (Fuel Cell Technologies, Inc.). The test was performed at 60 °C by feeding 2 or 5 M MeOH at a flow rate of 4 mL min^{-1} to the anode and humidified air (200 mL min^{-1}) to the cathode.

RESULTS AND DISCUSSION

Preparation and Characterization of Membranes. The preparation of the sandwich structured membranes was carried out in a three-step procedure of electrospinning, immobilizing PWA, and assembling the resulting sheet with two outer Nafion layers. Electrospinning technique was used to prepare beads free nanofiberous sheets with diameters in the range of 50−100 nm as shown in the SEM micrographs of electrospun fibers (Figure 1a and b). Self-anchoring of phosphotungstic acid resulted upon immersing of the nanofiberous sheet in PWA solution of desired concentration. Ion exchange capacity measurement of PWA anchored sheet revealed a value of as high as 4.1 (mequiv g^{-1}) and thermogravimetric analysis showed up to 55 wt % inorganic in 800 °C (as shown in Figure 2). This indicates that PWA immobilization as high as 54 wt % was achieved.

PWA comprise clusters of typically 12 W−O octahedral surrounding a central heteroatom. The IR spectrum of Keggin-type PWA (Figure S2) shows four characteristic bands at 1080 ($P-O_a$), 983 ($W = O_d$), 893 ($W-O_b-W$), and 797 ($W-O_c-W$) cm^{-1}. Upon anchoring onto nanofibers, the frequency of the peak correspond to the $W-O_c-W$ changes significantly (22 cm^{-1}). Smaller shift of 2 cm^{-1} to the lower frequency was also observed for the $W-O_b-W$ peak. So, it could be concluded that PWA is anchored due to the preferentially interactions reside at edge-sharing (O_c) and corner-sharing (O_b) oxygen sites rather than the terminal (O_d) site. In fact, these oxygen sites are preferred location of the Brønsted protons and DFT calculations with ^{31}P solid-state magic-angle-spinning NMR confirm these preferences.[37] Figure S3 shows FTIR spectra of the nanofibers before and after anchoring PWA. The changes on the characteristic peaks related to the PWA are highlighted and also summarized in Table S1. As shown, nylon anchored PWA possess inherent bands originated from both the substrate and PWA. A minor shift in the carbonyl frequency of the amide group (from 1636 to 1633 cm^{-1}) could be ascribed to the formation of hydrogen bonding with PWA.

Various sandwich structured membranes denoted as 3L membranes with a typical thickness of 75−95 μm was prepared thru assembling with two outer layers of recast Nafion using hot pressing. In order to enhance the adhesion between layers, Nafion solution was sprayed on the three components before assembling. A sandwich structure assembly of the membrane is shown clearly in the cross-sectional FESEM image in Figure 1d and 1e is a central layer. The surface image of the membrane (Figure 1f) confirms the nano size of dispersed PWA in the nanofibers matrix.

The fine dispersion of the PWA was confirmed using X-ray diffraction (XRD) pattern. As can be seen in Figure 3, none of

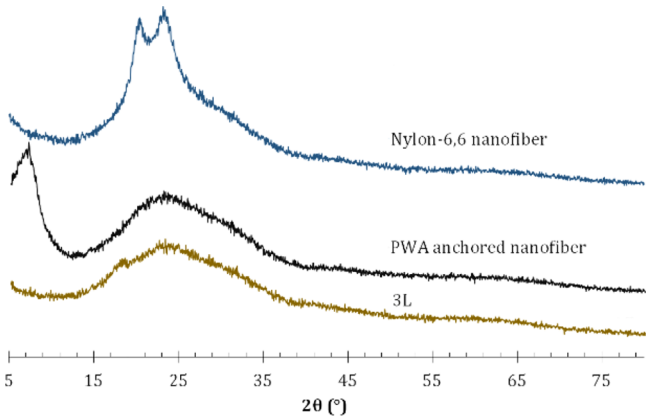

Figure 3. XRD patterns of the pristine nanofiber, PWA immobilized fiber, and 3L membrane.

the characteristic diffraction peaks of PWA (2θ: 11°, 15°, 19°, 23°, 27°, 31°, 37°, 40°, 44°, 56°, 63°, 65°) appeared in the PWA anchored nylon and 3L membrane even for 54 wt % PWA. The nanofiber shows the two strong diffraction peaks of (100) and (010, 110) corresponding to the α-phase crystals of typical triclinic form of nylons respectively at 2θ = 20.49° and 23.20°, respectively. The chains in this phase crystal are in fully extended planar conformation forming by hydrogen bonding. It must be pointed out that the reflections for nanofiber occur at a bit lower 2θ than value reported for pristine nylon. This feature suggest that the layers are farther apart and d-spacings of the electrospun fibers are enhanced in compare to casted nylon. However, interestingly, anchoring PWA to the nylon nanofiber transforms the α-phase into the new phase. Diffraction peaks of (100) and (010, 110) of nanofiber with spacing of 0.433 and 0.382 nm are replaced by one peak with a spacing of 0.385 nm centered at 23.06°. In addition, the pattern shows a new sharp peak at 2θ of 7.1°, which could be attributed to basal spacing indicating a layered structure with an interlayer distance of about 1.24 nm.

Proton Conductivity and Durability. Figure 4a shows the proton conductivities of 3L membranes of various thickness and PWA loading levels under fully hydrated conditions in the temperature range of 30−60 °C. As shown clearly, the conductivity enhanced as the PWA content increased in the central layer. Additionally, 3L membranes with thicker Nafion layers revealed higher proton conductivity and lower area resistance. A membrane containing PWA level of 51.12 wt % exhibited the lowest area resistance of 0.17 Ω cm^2 and highest proton conductivity of 5.8−7.8 × 10^{-2} S cm^{-1}, which are partially better than that of Nafion 115 under the same conditions. The plotted conductivity−temperature relationship showed Arrhenius type behavior in which the proton conductivity increased with the increase in the temperature. The activation energy (E_a) calculated from the slope of the conductivity curves, reveals that the E_a values of membranes with low PWA content are higher than that of Nafion (23.1 kJ mol^{-1} for 3L.3 compared to the 17.4 for N115). Interestingly, in a membrane with higher loading level of PWA the E_a even

DOI: 10.1021/acsami.5b02268
ACS Appl. Mater. Interfaces 2015, 7, 17008−17015

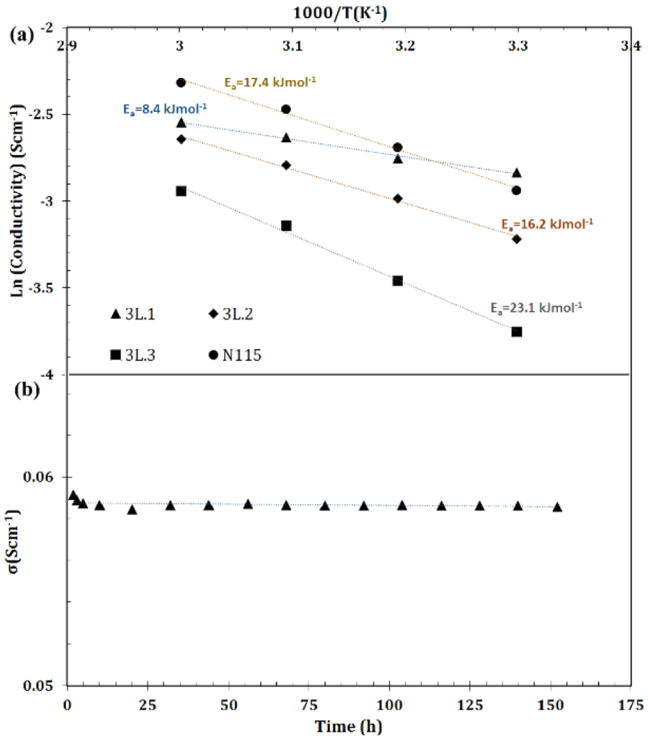

Figure 4. Temperature dependence of proton conductivity of composite membranes compared to Nafion 115 (a) and conductivity of 3L.1 membrane as a function of test time at 30 °C (b) showing the success of the designed membrane for addressing the PWA leaching.

drops to the values lower than 10 kJ mol^{-1}. This behavior can be attributed to the fact that higher concentration of the PWA in the central layer enhance the ability of protons to move between two highly conducting Nafion layers. Such low E_a along with high proton conductivity confirm a facile proton transport pathway in the sandwiched membranes. On the other hand, since the prepared membranes are anisotropic, it would be necessary to show the through-plane direction conductivity. As shown in the preliminary data in Table 1, despite the anisotropic morphology of the 3L membranes, the through-plane and in-plane conductivity are quite similar.

The durability of the proton conductivity was monitored by leaching test and further confirmed with measuring proton conductivity under fully hydrated condition for 150 h (Figure 4b). UV−vis data clearly showed that the leaching of PWA did not occur and proton conductivity plot displayed in Figure 3b showed that there is no obvious reduction in conductivity even after 150 h of continue testing. This data shows significant stability improvement upon simple mixing methods and surface modification of PWA/sulfonated polymer[38] or PWA-impregnated *meso*-Nafion multilayer[39] membranes, which were used and led to more than 18% decline in proton conductivity and 15.4 wt % reduction in the amount of PWA after 20 h immersing in water, respectively.

Methanol Permeability. To determine the performance of membranes in DMFC, the methanol permeability is evaluated and the selectivity was calculated as a ratio of proton conductivity to methanol permeability (σ/P). Linear correlation between methanol concentration and time was obtained and the permeability was calculated from the slope of linear fitted curves. A summary of the improvements to the methanol permeability and conductivity of the composite 3L membranes, compared with Nafion and highly selective composite membranes reported recently in the literature is shown in Table 1. Since the upper value of selectivity specifies the higher conductivity and lower permeability, better cell performance would be expected. As shown in Table 1, all multilayered membranes showed a drastically reduced methanol permeability (around 2 orders of magnitude). Beside this, the selectivity is almost 20 times greater than that of Nafion and the highly selective composite membranes reported recently. This data clearly confirm that the central layer composition and particularly the low intrinsic methanol permeability of nylon-66 play a main role in controlling the methanol crossover.

Excellent dimensional, chemical, and mechanical stabilities are required for ideal polyelectrolyte membranes because of their direct consequence on DMFC performance. Therefore, prior to in situ single cell testing, various stability examinations including dimensional changes upon swelling in water and water−methanol solutions and mechanical and chemical stabilities of the obtained membranes were performed and compared with Nafion 115. Table 2 shows the swelling ratio and water and methanol uptake as a function of temperature in the range of 30−60 °C. The 3L and Nafion 115 membranes exhibited an increased swelling ratios and water and methanol uptakes with the temperature increase. However, the swelling ratio and uptake value of the 3L membranes were lower than that of Nafion and the difference widen as the temperature

Table 1. PWA Loading Level, Thickness, Conductivities, Area Resistance, and Methanol Permeability and Selectivity of the Membranes at 30 °C

sample	thickness (μm)	proton conductivity [σ] (mS cm^{-1}) in-plane	proton conductivity [σ] (mS cm^{-1}) through-plane	area resistance (Ω cm^2)[a]	MeOH permeability [P] ($\times10^{-8}$ cm^2 s^{-1})	selectivity [$S = \sigma/P$] ($\times10^8$ mS·s cm^{-3})
3L.1 (51.12)[b]	95 (35−25−35)[c]	58.6	57.6	0.17	3.59	16.3
3L.2 (46.45)[b]	95 (35−25−35)[c]	40.0	38.9	0.24	3.02	13.2
3L.3 (46.45)[b]	75 (25−25−25)[c]	23.4	23.2	0.32	1.85	12.6
N115	127	52.9	52.4	0.24	104	0.51
L-*b*-L[d] onto nylon-6 nanofiber[20,40]	30		7.0	0.42	9.7	0.72
N212/PDDA-PWA[e41]	51					4.01

[a]Based on the through-plane measurements. [b]PWA loading level (%), indicated by thermal analysis. [c]Thickness of various layers (Nafion-central-Nafion). [d]Several layers of poly(diallyl dimethylammonium chloride)/sulfonated poly(2,6-dimethyl-1,4-phenylene oxide). [e]Four bilayers of poly(diallyl dimethylammonium chloride) and PWA.

DOI: 10.1021/acsami.5b02268
ACS Appl. Mater. Interfaces 2015, 7, 17008−17015

Table 2. Water and Methanol Uptake (ϕ_{w+MeOH}), In-Plane (S_{in}), Through-Plane (S_{tr}), and Volume (S_v) Swelling of the Membranes in 5 M Aqueous Methanol as a Function of Temperature

	Nafion 115				3L.1			
temperature (°C)	ϕ_{w+MeOH} (%)	S_{in} (%)	S_{tr} (%)	S_v (%)	ϕ_{w+MeOH} (%)	S_{in} (%)	S_{tr} (%)	S_v (%)
30	15.2	12.5	15.6	46.3	6.4	3.6	4.1	11.7
40	16.8	13.1	17.2	49.9	7.2	4.1	4.8	13.6
50	19.2	13.5	19.4	53.8	7.8	4.4	5.2	14.7
60	24.0	14.6	22.1	60.3	9.1	5.5	6.0	18.0

increased. Similar results were obtained for swelling and uptake in a pure water as reported in a Table S2 (Supporting Information). These observations are consistent with the results published by Horan et al.[35] who reported about 60% lower number of water molecules per H^+ of PWA based materials compared to Nafion and showing that this 3L film is considerably less dependent on water in achieving higher conductivity value than Nafion membrane.

The chemical stability of the membranes was evaluated by measuring the retained weight (RW) after 1, 5, and 24 h of immersion in Fenton's reagent as shown in the Table 3. 3L membrane remained intact and in reasonably good mechanical shape even after 24 h of testing. Compared to Nafion 115, the retained weight increased partially in the composite membrane. The enhanced chemical stability of the composite membrane is attributed to the presence of the PWA in the central layer, which is chemically stable. The elongation at break of the 3L.1 membrane was found to be lower than the Nafion 115 unlike the tensile strength which is comparable with that of Nafion 115 membrane.

Table 3. Chemical Stability Parameters of Membrane Dissolution and Retained Weight (RW) after 1, 5, and 24 h in Fenton's Reagent and Mechanical Properties of 3L.1 and Nafion 115

sample	RW_{1h} (wt %)	RW_{5h} (wt %)	RW_{24h} (wt %)	T_{dis}[a] (h)	tensile strength (MPa)	elongation at break (%)
3L.1	98.1	92.1	91.6	>96	20.8 ± 12	38.6 ± 2
N115	97.8	91.4	90.7	>96	22.6 ± 15	181.1 ± 4

[a]Dissolution time of membranes in Fenton's reagent.

Fuel Cell Performance of the 3-Layered Membrane. To demonstrate the suitability of the obtained highly conductive and methanol resistant membranes, DMFC tests were reported in comparison with Nafion 115 membrane. Figure 5 shows the power density and polarization curves of cells assembled with 3L.1 and Nafion based MEAs using 2 M (a) and 5 M (b) aqueous methanol feed at anode at 60 °C. It is noteworthy that although the proton conductivity of the 3L composite membranes is lower than that of Nafion 115 in 60 °C, the MEAs with 3L membrane showed better DMFC performance at both feed concentrations. Such higher performance could be attributed to the lower methanol crossover and better membrane selectivity. At 2 M methanol feed, the 3L.1 had an improvement in peak power of 49.6% above Nafion. However, more improvement in peak power by 113.3% was obtained with 5 M methanol feed as the maximum power density of 127.1 mW cm^{-2} that was observed for 3L membrane compared to 59.6 mW cm^{-2} for Nafion. Comparing the performance in various methanol concentrations as depicted in Figure 5 shows that although the maximum power density of Nafion is decreasing by 15% upon increasing feed concentration, it was increased by 21.4% for 3L membrane. This higher performance at increased feed concentration clearly

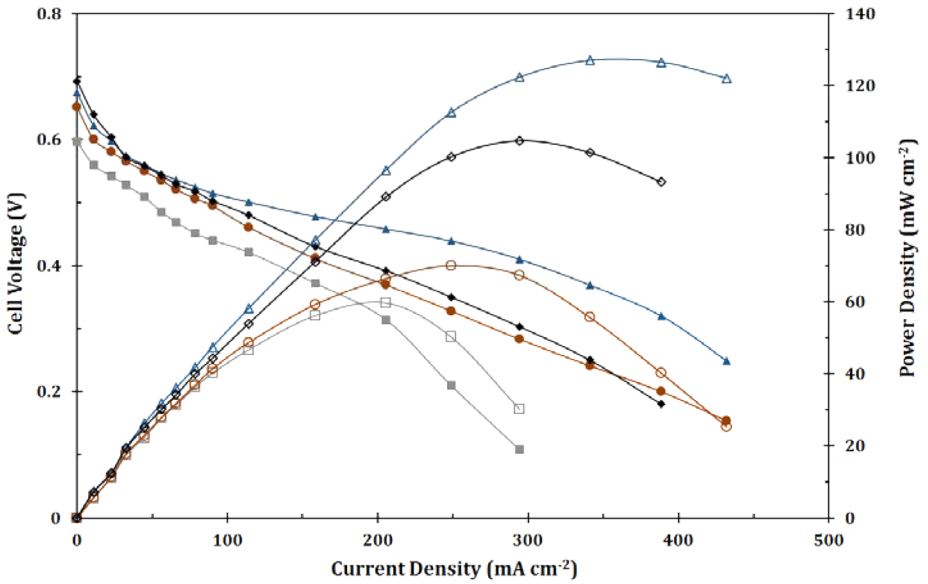

Figure 5. Polarization and power curves of DMFC single cell with Nafion 115 membrane (gray open circle, gray open box) and 3L.1 composite membrane (black open diamond, blue open triangle). Operating conditions of anode are 2 M (gray open circle, black open diamond) or 5 M (gray open box, blue open triangle) methanol, 4 mL min^{-1}.

DOI: 10.1021/acsami.5b02268
ACS Appl. Mater. Interfaces 2015, 7, 17008−17015

confirms the advantages of 3L membranes for DMFC with high methanol concentration. In addition, the OCV, which is directly related to the methanol crossover improved to 693 and 675 mV giving about 41 and 78 mV higher than that of Nafion 115 in 2 and 5 M methanol, respectively.

CONCLUSIONS

To prepare proton-conducting and methanol blocking layer for Nafion, high level of PWA was self-immobilized onto the electrospun nylon-66 nanofiberous sheet. This highly proton conductive sheet was assembled with 2 recast Nafion layers into composite membranes. In contrast with the conventional methods for Nafion modification, the self-immobilized PWA onto nylon fibrous sheet was found not only acts as an efficient methanol barrier layer but also imparts high and stable proton conductivity and better chemical and dimensional stabilities. Typically, the composite membrane exhibited the methanol permeability as low as 1.85×10^{-8} cm^2 s^{-1} and high through-plane proton conductivity of 23 mS cm^{-1} at 100% RH, indicating a membrane selectivity of 12.6×10^8 mS·s cm^{-3} which is around 20 times greater than the selectivity of Nafion. As a result, the 3L membrane proved up to 2 times better performance in DMFC single cell test compared to Nafion 115. In addition, while the peak power density of Nafion 115 was decreased at higher methanol concentration by 15%, the cell performance using 3L membrane increased remarkably as the peak power density increased by 21.4%. This improved performance in DMFC along with the excellent stability and selectivity, undetectable leaching of PWA and resulting durability of conductivity represents the potential of these composite membranes as a powerful candidate for applications at higher methanol concentrations.

ASSOCIATED CONTENT

Supporting Information

The Supporting Information is available free of charge on the ACS Publications website at DOI: 10.1021/acsami.5b02268.

Additional information and experimental data, including FTIR-ATR spectrum of PWA, nylon nanofiber, and anchored PWA on nylon and water swelling and uptake (PDF)

AUTHOR INFORMATION

Corresponding Author

*E-mail: ebrahim@utm.my. Phone/Fax: +60 (0)3 2615 4220.

Notes

The authors declare no competing financial interest.

ACKNOWLEDGMENTS

This research was funded by the This research was funded by the Malaysian Ministry of Higher Education and Universiti Teknologi Malaysia under Research University Fund Scheme (vote no.#10H39) and LRGS program (vote no.#4L817).

REFERENCES

(1) Kreuer, K.-D. Ion Conducting Membranes for Fuel Cells and other Electrochemical Devices. *Chem. Mater.* **2014**, *26* (1), 361−380.
(2) Nasef, M. M. Radiation-Grafted Membranes for Polymer Electrolyte Fuel Cells: Current Trends and Future Directions. *Chem. Rev.* **2014**, *114* (24), 12278−12329.
(3) Hickner, M. A.; Ghassemi, H.; Kim, Y. S.; Einsla, B. R.; McGrath, J. E. Alternative Polymer Systems for Proton Exchange Membranes (PEMs). *Chem. Rev.* **2004**, *104* (10), 4587−4612.
(4) Li, X.; Faghri, A. Review and Advances of Direct Methanol Fuel Cells (DMFCs) Part I: Design, Fabrication, and Testing with High Concentration Methanol Solutions. *J. Power Sources* **2013**, *226* (0), 223−240.
(5) Mochizuki, T.; Uchida, M.; Uchida, H.; Watanabe, M.; Miyatake, K. Double-Layer Ionomer Membrane for Improving Fuel Cell Performance. *ACS Appl. Mater. Interfaces* **2014**, *6* (16), 13894−13899.
(6) Roziere, J.; Jones, D. J. Non-Fluorinated Polymer Materials for Proton Exchange Membrane Fuel Cells. *Annu. Rev. Mater. Res.* **2003**, *33*, 503−555.
(7) Argun, A. A.; Ashcraft, J. N.; Hammond, P. T. Highly Conductive, Methanol Resistant Polyelectrolyte Multilayers. *Adv. Mater.* **2008**, *20* (8), 1539−1543.
(8) Lobato, J.; Cañizares, P.; Rodrigo, M. A.; Linares, J. J.; López-Vizcaíno, R. Performance of a Vapor-Fed Polybenzimidazole (PBI)-Based Direct Methanol Fuel Cell. *Energy Fuels* **2008**, *22* (5), 3335−3345.
(9) Gubler, L.; Kramer, D.; Belack, J.; Ünsal, Ö.; Schmidt, T. J.; Scherer, G. G. Celtec-V: a Polybenzimidazole-Based Membrane for the Direct Methanol Fuel Cell. *J. Electrochem. Soc.* **2007**, *154* (9), B981−B987.
(10) Pandey, R. P.; Thakur, A. K.; Shahi, V. K. Sulfonated Polyimide/Acid-Functionalized Graphene Oxide Composite Polymer Electrolyte Membranes with Improved Proton Conductivity and Water-Retention Properties. *ACS Appl. Mater. Interfaces* **2014**, *6* (19), 16993−17002.
(11) Awang, N.; Ismail, A. F.; Jaafar, J.; Matsuura, T.; Junoh, H.; Othman, M. H. D.; Rahman, M. A. Functionalization of Polymeric Materials as a High Performance Membrane for Direct Methanol Fuel Cell: a Review. *React. Funct. Polym.* **2015**, *86* (0), 248−258.
(12) Sanchez, C.; Belleville, P.; Popall, M.; Nicole, L. Applications of Advanced Hybrid Organic-Inorganic Nanomaterials: from Laboratory to Market. *Chem. Soc. Rev.* **2011**, *40* (2), 696−753.
(13) Cavaliere, S.; Subianto, S.; Savych, I.; Jones, D. J.; Roziere, J. Electrospinning: Designed Architectures for Energy Conversion and Storage Devices. *Energy Environ. Sci.* **2011**, *4* (12), 4761−4785.
(14) Ballengee, J. B.; Pintauro, P. N. Morphological Control of Electrospun Nafion Nanofiber Mats. *J. Electrochem. Soc.* **2011**, *158* (5), B568−B572.
(15) Ballengee, J. B.; Pintauro, P. N. Composite Fuel Cell Membranes from Dual-Nanofiber Electrospun Mats. *Macromolecules* **2011**, *44* (18), 7307−7314.
(16) Li, H.-Y.; Liu, Y.-L. Nafion-Functionalized Electrospun Poly(vinylidene fluoride) (PVDF) Nanofibers for High Performance Proton Exchange Membranes in Fuel Cells. *J. Mater. Chem. A* **2014**, *2* (11), 3783−3793.
(17) Sharma, D. K.; Shen, J.; Li, F. Reinforcement of Nafion into Polyacrylonitrile (PAN) to Fabricate them into Nanofiber Mats by Electrospinning: Characterization of Enhanced Mechanical and Adsorption Properties. *RSC Adv.* **2014**, *4* (74), 39110−39117.
(18) Tamura, T.; Kawakami, H. Aligned Electrospun Nanofiber Composite Membranes for Fuel Cell Electrolytes. *Nano Lett.* **2010**, *10* (4), 1324−1328.
(19) Subramanian, C.; Weiss, R. A.; Shaw, M. T. Fabrication and Characterization of Conductive Nanofiber-Based Composite Membranes. *Ind. Eng. Chem. Res.* **2013**, *52* (43), 15088−15093.
(20) Liu, D. S.; Ashcraft, J. N.; Mannarino, M. M.; Silberstein, M. N.; Argun, A. A.; Rutledge, G. C.; Boyce, M. C.; Hammond, P. T. Spray Layer-by-Layer Electrospun Composite Proton Exchange Membranes. *Adv. Funct. Mater.* **2013**, *23* (24), 3087−3095.
(21) Sailaja, G. S.; Zhang, P.; Anilkumar, G. M.; Yamaguchi, T. Aniosotropically Organized LDH on PVDF: A Geometrically Templated Electrospun Substrate for Advanced Anion Conducting Membranes. *ACS Appl. Mater. Interfaces* **2015**, *7* (12), 6397−6401.
(22) Won, J.-H.; Lee, H.-J.; Lim, J.-M.; Kim, J.-H.; Hong, Y. T.; Lee, S.-Y. Anomalous Behavior of Proton Transport and Dimensional Stability of Sulfonated Poly(arylene ether sulfone) Nonwoven/Silicate

DOI: 10.1021/acsami.5b02268
ACS Appl. Mater. Interfaces 2015, 7, 17008−17015

Composite Proton Exchange Membrane with Dual Phase Co-continuous Morphology. *J. Membr. Sci.* **2014**, *450* (0), 235−241.
(23) Wang, L.; Zhu, J.; Zheng, J.; Zhang, S.; dou, L. Nanofiber Mats Electrospun from Composite Proton Exchange Membranes Prepared from Poly(aryl ether sulfone)s with Pendant Sulfonated Aliphatic Side Chains. *RSC Adv.* **2014**, *4* (48), 25195−25200.
(24) Lin, Z.; Yao, Y.; Zhang, X. Electrospun Nanofibers for Design and Fabrication of Electrocatalysts and Electrolyte Membranes for Fuel cells. In *Electrospun Nanofibers for Energy and Environmental Applications*; Ding, B.; Yu, J., Eds.; Springer: Berlin, 2014; pp 41−67.
(25) Cavani, F. Heteropolycompound-based Catalysts: a Blend of Acid and Oxidizing Properties. *Catal. Today* **1998**, *41* (1−3), 73−86.
(26) Wu, H.; Shen, X.; Cao, Y.; Li, Z.; Jiang, Z. Composite Proton Conductive Membranes Composed of Sulfonated Poly(ether ether ketone) and Phosphotungstic Acid-loaded Imidazole Microcapsules as Acid Reservoirs. *J. Membr. Sci.* **2014**, *451* (0), 74−84.
(27) Xiang, Y.; Yang, M.; Zhang, J.; Lan, F.; Lu, S. Phosphotungstic Acid (HPW) Molecules Anchored in the Bulk of Nafion as Methanol-blocking Membrane for Direct Methanol Fuel Cells. *J. Membr. Sci.* **2011**, *368* (1−2), 241−245.
(28) Bose, A. B.; Gopu, S.; Li, W. Enhancement of Proton Exchange Membrane Fuel Cells Performance at Elevated Temperatures and Lower Humidities by Incorporating Immobilized Phosphotungstic Acid in Electrodes. *J. Power Sources* **2014**, *263* (0), 217−222.
(29) Lu, J. L.; Fang, Q. H.; Li, S. L.; Jiang, S. P. A Novel Phosphotungstic acid Impregnated meso-Nafion Multilayer Membrane for Proton Exchange Membrane Fuel Cells. *J. Membr. Sci.* **2013**, *427* (0), 101−107.
(30) Malhotra, S.; Datta, R. Membrane-supported Nonvolatile Acidic Electrolytes Allow Higher Temperature Operation of Proton-Exchange Membrane Fuel Cells. *J. Electrochem. Soc.* **1997**, *144* (2), L23−L26.
(31) Shao, Z.-G.; Xu, H.; Li, M.; Hsing, I. M. Hybrid Nafion−inorganic Oxides Membrane Doped with Heteropolyacids for High Temperature Operation of Proton Exchange Membrane Fuel Cell. *Solid State Ionics* **2006**, *177* (7−8), 779−785.
(32) Ramani, V.; Kunz, H. R.; Fenton, J. M. Investigation of Nafion®/HPA Composite Membranes for High Temperature/Low Relative Humidity PEMFC Operation. *J. Membr. Sci.* **2004**, *232* (1−2), 31−44.
(33) Herring, A. M. Inorganic−Polymer Composite Membranes for Proton Exchange Membrane Fuel Cells. *J. Macromol. Sci., Polym. Rev.* **2006**, *46* (3), 245−296.
(34) Horan, J. L.; Genupur, A.; Ren, H.; Sikora, B. J.; Kuo, M.-C.; Meng, F.; Dec, S. F.; Haugen, G. M.; Yandrasits, M. A.; Hamrock, S. J.; Frey, M. H.; Herring, A. M. Copolymerization of Divinylsilyl-11-silicotungstic Acid with Butyl Acrylate and Hexanediol Diacrylate: Synthesis of a Highly Proton-Conductive Membrane for Fuel-Cell Applications. *ChemSusChem* **2009**, *2* (3), 226−229.
(35) Horan, J. L.; Lingutla, A.; Ren, H.; Kuo, M.-C.; Sachdeva, S.; Yang, Y.; Seifert, S.; Greenlee, L. F.; Yandrasits, M. A.; Hamrock, S. J.; Frey, M. H.; Herring, A. M. Fast Proton Conduction Facilitated by Minimum Water in a Series of Divinylsilyl-11-silicotungstic Acid-co-Butyl Acrylate-co-Hexanediol Diacrylate Polymers. *J. Phys. Chem. C* **2014**, *118* (1), 135−144.
(36) Abouzari-Lotf, E.; Ghassemi, H.; Shockravi, A.; Zawodzinski, T.; Schiraldi, D. Phosphonated Poly(arylene ether)s as Potential High Temperature Proton Conducting materials. *Polymer* **2011**, *52* (21), 4709−4717.
(37) Feng, N.; Zheng, A.; Huang, S.-J.; Zhang, H.; Yu, N.; Yang, C.-Y.; Liu, S.-B.; Deng, F. Combined Solid-State NMR and Theoretical Calculation Studies of Brønsted Acid Properties in Anhydrous 12-Molybdophosphoric Acid. *J. Phys. Chem. C* **2010**, *114* (36), 15464−15472.
(38) Xu, D.; Zhang, G.; Zhang, N.; Li, H.; Zhang, Y.; Shao, K.; Han, M.; Lew, C. M.; Na, H. Surface Modification of Heteropoly Acid/SPEEK Membranes by Polypyrrole with a Sandwich Structure for Direct Methanol Fuel Cells. *J. Mater. Chem.* **2010**, *20* (41), 9239−9245.
(39) Lu, J. L.; Fang, Q. H.; Li, S. L.; Jiang, S. P. A novel phosphotungstic acid impregnated meso-Nafion multilayer membrane for proton exchange membrane fuel cells. *J. Membr. Sci.* **2013**, *427* (0), 101−107.
(40) Mannarino, M. M.; Liu, D. S.; Hammond, P. T.; Rutledge, G. C. Mechanical and Transport Properties of Layer-by-Layer Electrospun Composite Proton Exchange Membranes for Fuel Cell Applications. *ACS Appl. Mater. Interfaces* **2013**, *5* (16), 8155−8164.
(41) Yang, M.; Lu, S.; Lu, J.; Jiang, S. P.; Xiang, Y. Layer-by-layer Self-Assembly of PDDA/PWA-Nafion Composite Membranes for Direct Methanol Fuel Cells. *Chem. Commun.* **2010**, *46* (9), 1434−1436.

DOI: 10.1021/acsami.5b02268
ACS Appl. Mater. Interfaces 2015, 7, 17008−17015